Validation of GNSS-Based High-Precision Velocity Estimation for Outdoor Sports

Geo BOFFI, Switzerland,Matthias GILGIEN, Norway
Andreas WIESER, Switzerland

Key words: GNSS, Velocity Estimation, Doppler Observations, Photocells

SUMMARY

GNSS can provide three-dimensional velocity of a mobile user with mm/s accuracy, and with high temporal and spatial resolution. This is facilitated in particular using Doppler observables computed as first-order central differences from the carrier-phase and it does not require use of a high-end receiver.

In certain outdoor sports it is desired to capture the trajectory and the dynamics of an athlete with high temporal and spatial resolution, and possibly also high accuracy. This is primarily for training, detailed performance analysis, studying risk, and for research while ranking during competition is typically based on time measurements e.g., using photocells. Due to the virtually unlimited operation range and the inherent capability of yielding location, velocity and time, GNSS receivers are particularly well suited for the above purposes.

In this paper we present models for predicting the accuracy of both GNSS-derived and photocell-based speed estimates, showing that generally the GNSS-based estimates will be significantly more accurate if GNSS is available. We have validated the models using data from tests on a coaster track which mimicked the dynamics of outdoor sports potentially benefitting from the technology and at the same time allowed repetition under reasonably controlled conditions.

The results confirmed that a precision better than 10 mm/s can be obtained for the instantaneous speed estimate provided by a consumer-grade receiver and that even better accuracy is obtained by temporal averaging since the data are sufficiently uncorrelated. The high-end geodetic receiver, also used in the tests, was found to be less suitable. While the results directly refer to a specific application the findings are more generally valid and may also be useful for a variety of other applications involving motion capture with kinematic GNSS receivers.

Validation of GNSS-Based High-Precision Velocity Estimation for Outdoor Sports

Geo BOFFI, Switzerland,Matthias GILGIEN, Norway
Andreas WIESER, Switzerland

1. INTRODUCTION

In many outdoor sports performance is measured in time and it is a function of path length and velocity along the path. The ranking in competition is typically achieved by measuring time using photocell systems, and velocity is only determined as an additional information. However, for training, detailed performance analysis, studying risk, and for research it may be required to get more information. In sports where the path length is equal for each athlete (e.g. athletic sprinting) velocity is usually determined using photocell systems (Yeadon et al., 1999). When the paths are different between athletes both path and velocity, possibly also further parameters, need to be determined to allow comprehensive insight in determinants of performance (Federolf, 2012; Gilgien, 2016). In certain sports video systems (Klous et al., 2010; Reid, 2010; Spörri et al., 2012) or infrared light based photogrammetric systems (Nedergaard et al., 2013; Lindinger, 2007) are applied to reconstruct the center of mass trajectory and to derive the velocity. Such systems are accurate and rich in information (segment movements), but limited to small capture volumes because they are complex in their application and expensive in terms of time and resources. In court based sports ultra sound based systems (Fontana, 2002) or radio based systems (Leser et al., 2011) are used as an alternative. For sports which are exerted across large spatial volumes GNSS (Lachapelle, 2009; Gilgien, 2013, 2015) or a combination of GNSS and inertial systems (Skaloud and Limpach, 2003; Supej, 2010) are applied. Challenges arising in this context are typically found in all kinematic applications of GNSS, and tools well established in surveying are suitable to analyze and mitigate them.

Using GNSS the velocity over ground can be determined from the time tagged estimated positions along the trajectory or directly from Doppler observables (Kaplan et al., 2006). Highly precise Doppler observables can be computed from the carrier-phase output (Ward et al., 2006) and used for the estimation of velocity time series which are more precise than those estimated either from the raw Doppler measurements of the receiver or calculated from position solutions (Wieser, 2007). The feasibility of GNSS based velocity estimation with mm/s accuracy has been shown even using low-cost, consumer-grade GNSS receivers, see e.g. Wieser (ibid); Ford and Hamilton (2003); Zang et al. (2006).

Several studies reported mean errors of GNSS based velocity measurements for sport applications ranging from 0.3 to 0.02 m/s (Supej and Holmberg, 2011; Boffi, 2013; Supej and Cuk, 2014, Gilgien, 2014) and demonstrated potential of this technology for applications in sport. These studies typically involved photocells at known distances as reference system, but the photocells were actually triggered by the athletes not by the GNSS receivers. So there was a varying time difference between the triggering and the passage of the GNSS antenna, and the results of the studies were

neither corrected for these offsets nor was the resulting uncertainty quantified and taken into account. In other cases the reached velocities and dynamics were not comparable to the real sports situations (Supej and Holmberg, ibid).

In this study accurate Doppler observables are derived from carrier-phase measurements of two different receivers (a consumer-grade one and a high-end geodetic one) and used to determine the velocity. Accuracy assessment is carried out using photocells but the measurements are made on a rail-guided sled and thus within a setting where path length and trigger time were controlled and repeatable. Sled speed and GNSS-obstruction by the surroundings were typical for sport applications like alpine skiing. The uncertainty of all measurements is taken into account for the validation.

2. METHOD

2.1 GNSS-based velocity computation

The Doppler shift f_d of the GNSS signals is proportional to the relative velocity between satellite and receiver along the line-of-sight. The highly precise carrier-phase observation within the receiver is a measurement of integrated Doppler shift. Therefore, highly precise Doppler shift can be obtained by approximating the time-derivative of the carrier phase e.g., using the first order central difference (Wieser 2007, p.16 ff.):

$$f_d(t_i) := \frac{\Phi(t_{i+1}) - \Phi(t_{i-1})}{2\Delta t} \approx f_0 \cdot \frac{v(t_i)}{c} \qquad (1)$$

where $2\Delta t$ is the time difference between epochs t_{i-1} and t_{i+1}, $\Phi(t_i)$ is the carrier-phase at epoch i, f_0 is the transmitted frequency, c is the wave propagation speed and v is the relative velocity between transmitter and receiver along the line of sight. For the application discussed herein the approximation according to (1) is sufficiently accurate to achieve mm/s level accuracy and all results reported later on are based on this "Doppler observable" rather than on the Doppler observable directly output by the receivers (which is based on the receiver's frequency-lock-loop and has an accuracy on the dm/s- to m/s-level).

The observed Doppler shift f_d is related to the velocity vector $\mathbf{v}_r$ of the receiver:

$$f_d - \frac{1}{\lambda}\mathbf{v}_s^T\mathbf{a} - f_0\dot{b_s} = \frac{1}{\lambda}\mathbf{a}^T\mathbf{v}_r - f_0\dot{b_r} + \varepsilon \qquad (2)$$

The satellite velocity vector $\mathbf{v_s}$, the satellite clock drift $\dot{b_s}$, the receiver-to-satellite unit vector $\mathbf{a}$ and the carrier wave length λ are either known or can be computed with sufficient accuracy using the broadcast or predicted orbit data, and position/time calculated by the receiver. The receiver clock drift $\dot{b_r}$ is unknown and needs to be estimated along with the three components of $\mathbf{v}_r$. This can be achieved using simultaneous Doppler measurements from at least four satellites, in a way perfectly equivalent to position and time determination using pseudoranges (Kaplan et al., 2006).

Herein, the observations are processed kinematically in an Extended Kalman Filter with receiver motion modelled as velocity random walk.[1] The corresponding spectral noise density has been set high (q = 1 m^2/s^3) compared to observation noise and anticipated actual velocity changes, which results in nearly unfiltered epoch-by-epoch solutions.

Analyzing the accuracy of the estimated velocities is straightforward if the true velocity is known exactly. This is very difficult to achieve for a kinematic GNSS receiver but easy for a static one. Many effects, like satellite orbit deviations, clock instabilities, or atmospheric propagation delays are independent of receiver motion; multipath effects are compressed in time but preserved in amplitude with slow receiver motion, and mitigated by the loop-filters of the receiver with fast receiver motion. Only the level of random observation noise will most likely be somewhat higher for a kinematic receiver than a static one (Wieser 2007, p.101 ff.), but random noise is not the dominant noise contribution. So we expect that a static test provides a useful indication of the precision $\sigma_{v,GNSS}$ of the receiver velocity determined from GNSS observations. Fig. 1 shows the results of such a test for a consumer-grade GPS receiver (u-blox EVK6T) in an unobstructed area with a 5 Hz data rate. The RMSE of the 3D velocity (speed) $\|\mathbf{v}_r\|$ is 8.5 mm/s. An analog experiment was performed using a high-end geodetic GPS receiver (Leica GX1230GG) resulting in a RMSE of 3.5 mm/s.

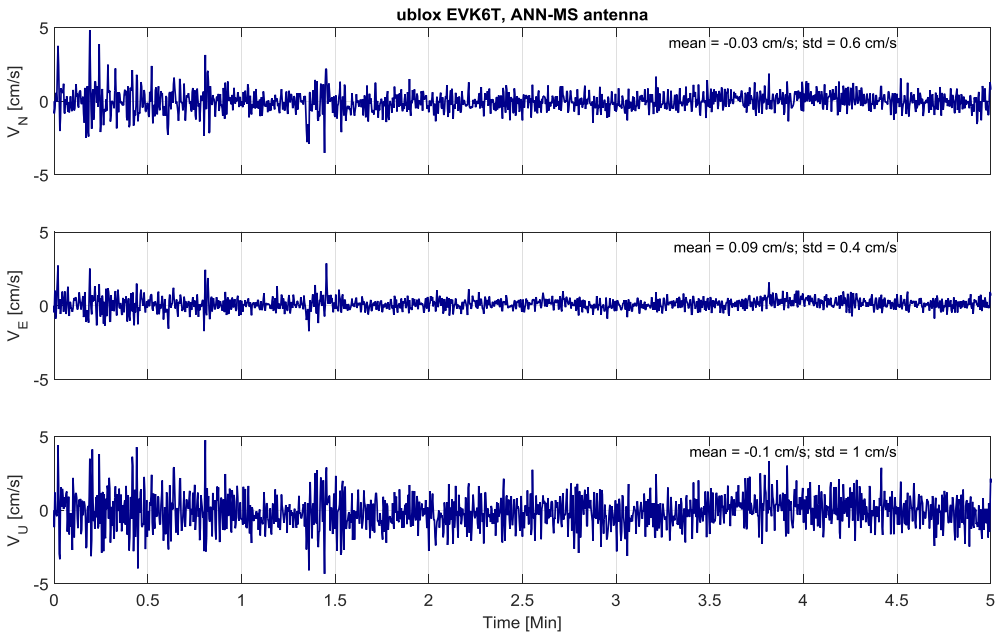

Figure 1: Time series of estimated velocity components (North, East, Up) of actually static antennas and 5 Hz measurement rate using consumer-grade. An analog experiment was performed using a high-end receiver; data processing see text.

[1] A proprietary MATLAB software (KF_run) has been used for this purpose.

A correlation analysis of the results has shown that they are practically uncorrelated between epochs at this data rate. So we can calculate the standard deviation of the mean velocity over *n* epochs from the one of the single-epoch values as:

$$\sigma_{\bar{v},G} = \frac{1}{\sqrt{n}}\sigma_{v,G} \tag{3}$$

The performance with kinematic receiver will be assessed by collecting measurements with the receiver travelling repeatedly along a reproducible trajectory and comparing the estimated velocities to reference values obtained independently.

2.2 Reference Measurements

We use a photocell based measurement system to obtain the reference measurements for the experimental investigation with kinematic GPS receivers. The photocell system consists of a series of nodes, each of them composed of a sender emitting a continuous light beam, a reflector and a receiver. Each node detects interruptions of the light beam and thus records the transit time *t* of an object through the beam. If the travelled distance $d_{i,j}$ between two photocells *i* and *j* is known, the mean speed $\bar{v}_{i,j}^{p}$ between these photocells follows from:

$$\bar{v}_{i,j}^{p} = \frac{d_{i,j}}{(t_j - t_i)} \tag{4}$$

With the aid of variance propagation we can estimate the standard deviation of this mean speed. Assuming that the three involved measurements (two transit times, a distance) are independent, we get:

$$\sigma_{\bar{v}_{i,j}^{p}} = \sqrt{\left(\frac{\partial \bar{v}_{i,j}^{p}}{\partial t_i}\right)^2 \cdot \sigma_{t_i}^2 + \left(\frac{\partial \bar{v}_{i,j}^{p}}{\partial t_j}\right)^2 \cdot \sigma_{t_j}^2 + \left(\frac{\partial \bar{v}_{i,j}^{p}}{\partial d_{i,j}}\right)^2 \cdot \sigma_{d_{i,j}}^2} \tag{5}$$

where $\sigma_{t_i}^2$ is the standard deviation of the transit time recorded by the *i*-th photocell, and $\sigma_{d_{i,j}}^2$ is that of the distance. Calculating the partial derivatives of (4) and assuming that the transit time measurement has the same standard deviation $\sigma_t$on all nodes, we obtain:

$$\sigma_{\bar{v}_{i,j}^{p}} = \frac{1}{t_j - t_i}\sqrt{2 \cdot \left(\bar{v}_{i,j}^{p}\sigma_t\right)^2 + \sigma_{d_{i,j}}^2} = \frac{\bar{v}_{i,j}^{p}}{d_{i,j}}\sqrt{2 \cdot \left(\bar{v}_{i,j}^{p}\sigma_t\right)^2 + \sigma_{d_{i,j}}^2} \tag{6}$$

Based on technical data provided by the manufacturers of the chosen photocells[2], the time resolution of the photocell devices is $r_t \leq 0.125$ ms. Therefore, we approximate the standard deviation of the time measurements as:

$$\sigma_t \cong \frac{1}{3} r_t = 0.041 \text{ ms} \qquad (7)$$

Assuming that we can determine the distance travelled between subsequent photocells with a standard deviation of 2 cm, we can now calculate the expected standard deviation of the mean speed using (6). It depends on mean speed and distances between the photocells. Results of the analysis are plotted in Fig. 3 which helps to choose suitable distances between the photocells such that the standard deviation of the reference measurements is as close as possible to the standard deviation of the GPS results. Ideally, the reference values should be significantly more accurate than the test values. However, as can be seen from the figure, this is not possible for the expected speed of up to 16 m/s and assuming that the previously determined RMSE of the GPS-based speed estimates from the static test (8.5 mm/s and 3.5 mm/s at 5 Hz) is also achieved in the kinematic test. Depending on speed and distance between the photocells the GPS receiver may travel between the photocells for several seconds and thus the GPS-derived speed needed for comparison will be an average speed over several epochs with standard deviation significantly better than 8.5 mm/s according to (3). The test will still be useful, but we clearly need to take into account also the uncertainty of the photocell measurements when assessing the results.

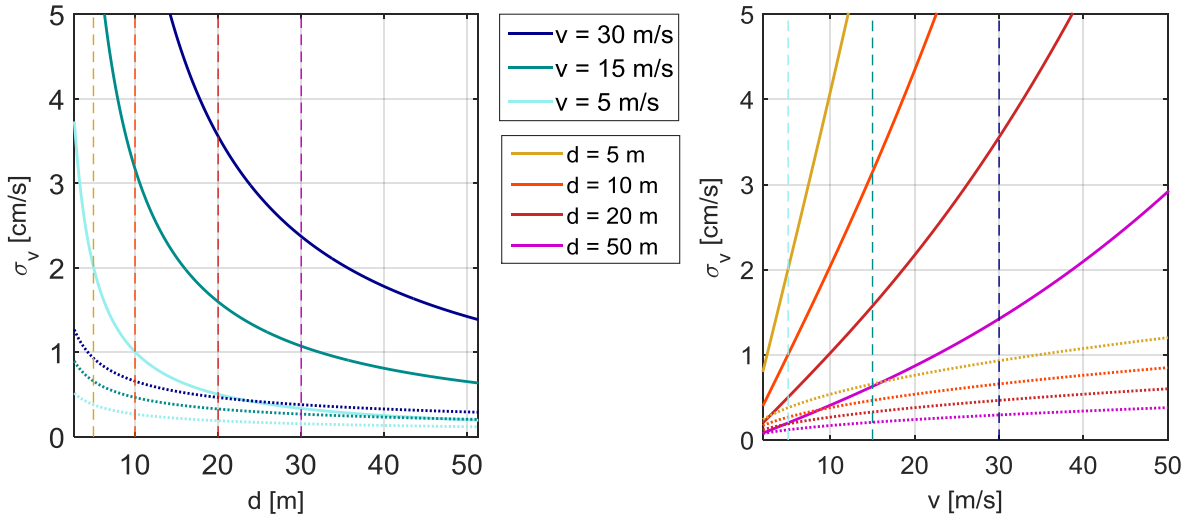

Figure 2: Standard deviation of photocell-based speed measurements as function of average speed v and distance d between photocells (bold lines), expected standard deviation of GPS-derived average speed (consumer-grade receiver) between photocells (pointed line). The dashed lines refer to the velocity on the distance-based plot and vice versa. Further assumptions, see text.

2.3 Kinematic test measurements

[2] Microgate POLIFEMO (http://www.microgate.it/Timing/Products/Photocells/Polifemo/Data-Sheet-for-all-Polifemo) and ALGE Timing Photocell PR1a (http://www.alge-timing.com/alge-e.htm)

We carried out the test measurements on a coaster track in the Swiss Alps (see Fig. 3). As a compromise between accuracy and spatial resolution we have decided to place the photocells at distances varying between 3 m and 12 m along the track. Ideally the whole track, in particular also the part through the forest, would have been equipped with photocells. However, due to limited availability of cells and effort for setting up we had to restrict the experiment to a short subsection for which we chose the part allowing highest maximum speed. This resulted in a validation section of 51.2 m length which was equipped with 9 photocells. The two GPS receivers mentioned previously were connected to their respective antennas which in turn were rigidly mounted on a coaster car (Fig. 4). Raw GPS data were collected at a 5 Hz data rate. Six runs were performed, with speeds between 45 km/h and 56 km/h in the validation section.

With this setup and location we achieved several objectives required for the goal of this investigation:

- The travelled distance between the photocells should be known with an accuracy of a few cm.
- The relation between the GPS antenna and the moving part triggering the photocells should be known and stable over time.
- The experiment should be repeatable.
- The distance between the photocells should balance sufficient accuracy of the reference measurements (long distance, see Fig. 2) and representativeness of the average speed for dynamic situations (short distance).
- The dynamics of the body carrying the GPS receivers should be similar to those in outdoor sports like downhill skiing.

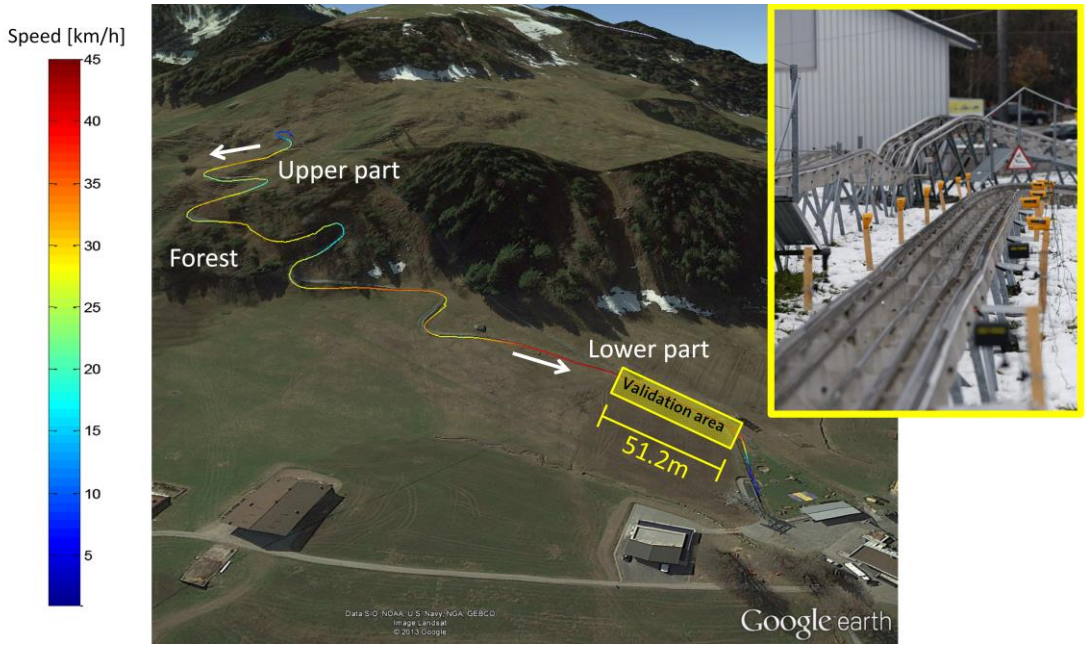

Figure 3: Trajectory of the downhill part of the coaster track, with validation area covering its lower part, GNSS-derived speed for a representative run (rainbow colors); photocells set up along the track (insert).

Figure 4: Coaster car with both GNSS antennas fixed on the front part; microwave absorbing foam was used to reduce potential signal reflections from the car's nearby metal parts.

The longitudinal axis of the track and the exact locations of the connection lines between each photocell's receiver/transmitter and reflector were measured before the test run using a high-end totalstation that yields mm-level accuracy of the individual coordinates determined. The track was then approximated using spline interpolation and the track points measured with the totalstation. Finally, the travelled distances between the photocells, later to be used in the calculation of the mean velocities, were calculated from the longitudinal axis and the above connecting lines assuming that the cells are triggered by an opaque rectangle moving along the track axis with its triggering edge al-

ways orthogonal to the track axis and within a vertical plane. In reality the front bumper of the car would trigger the photocells, and the above rectangle is an approximation to the longitudinal cross section of the bumper.

The photocell system was synchronized with GPS time. Using the time series of the GPS-based speed estimates, the respective average speed was calculated for each time interval between two photocell trigger events. Thus for each run average speed was calculated for 36 pairs of photocells (all pairs out of 9 cells[3]) from both GPS and photocell measurements. For each of these pairs, the expected standard deviation $\sigma_{\Delta v}$ of the difference Δv between the mean speed $\bar{v}_{\mathrm{G}}$ obtained from GPS and the mean speed $\bar{v}_p$ obtained from the photocells was calculated:

$$\Delta v = \bar{v}_G - \bar{v}_p \tag{8}$$

$$\sigma_{\Delta v} = \sqrt{\sigma_{\bar{v},G}^2 + \sigma_{\bar{v},p}^2} \tag{9}$$

3. RESULTS AND DISCUSSION

A typical velocity profile of the downhill run on the coaster track is shown in Fig. 5a for both GPS receivers. Fig. 5b shows the respective number of tracked satellites. The coaster track can be divided in four parts (Fig. 5c): (i) the ascent with constant speed, (ii) the upper part with little signal obstructions, (iii) the thick forest with strong signal obstructions, and (iv) the final part with good satellite availability. The validation section is located in part (iv).

Consumer-grade receivers are typically optimized for fast signal acquisition and tracking of weak signals (at the cost of potentially lower signal quality), while high-end geodetic receivers are optimized for quality (Wieser et al., 2005). This is well reflected by our results: the consumer-grade receiver yields much more signals in the obstructed area (Fig. 5b) and the estimated speed is plausible along the whole track (though noisy within the forest). The high-end receiver has less than 4 satellites for some time, during which the estimated speed is heavily based on prediction within the filter and thus poorly reflects the true motion. It is worth mentioning that the forest section here (Fig.5c, iii) causes stronger signal disturbances than expected for typical skiing environment where forest may still limit the signal reception but the slope is wider than the coaster track and thus less of the sky will be obstructed than during the "forest" section of our experiment.

The differences between $\bar{v}_p$ and $\bar{v}_{\mathrm{G}}$ are plotted in Fig. 6 (+) for both receivers, for all 6 runs and for all pairs of photocells. For each distance between photocells, the mean value and RMSE of the respective speed differences was also calculated and plotted (Fig. 6, squares and shaded areas). Finally, the standard deviation of the differences was predicted (dashed lines) as a function of distance

[3] The samples thus obtained are of course correlated, but striving for uncorrelated data would have meant restricting to only 4 pairs per run. For some of the analysis later only uncorrelated samples from all available pairs are selected.

using eqs. (9), (6) and (3), and a fixed speed of 15 m/s which is close to the maximum speed observed in the validation section during the 6 runs.

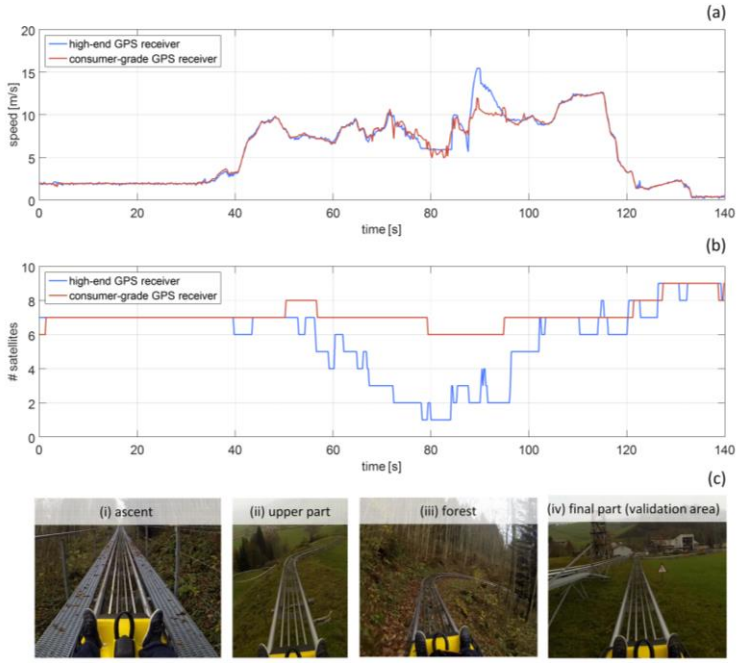

Figure 5: (a) Velocity profile during a run measured with a consumer-grade and a high-end GNSS receiver. (b) Comparison of the satellite availability during the run tracked using a consumer-grade and a high-end GNSS receiver. (c) Description of the four parts of the track.

Fig. 6 indicates that the predicted and experimentally determined precision match well for the consumer-grade receiver (right plot) while the results obtained using the high-end receiver (left plot) were clearly worse than the prediction, and also worse than those of the consumer-grade receiver. Since the data were obtained from the same runs for both receivers, this indicates that indeed the high-end receiver in its used configuration was not as appropriate for the task as the other one. Apart from the faster signal acquisition capability and higher sensitivity the loop filter settings of the consumer-grade receiver are very likely more suitable for the present kinematic application than those of the high-end receiver while the dual-frequency capability and the lower noise level of the latter are not required in this case.

A closer look at Fig. 6 shows that still the prediction seems to be slightly too optimistic in particular for longer distances. However, it is not possible to further analyze this using the available data, because the RMSE values are correlated across distances due to the correlations mentioned earlier (calculation of 36 differences from only 9 original time measurements per run).[4] We think that the reason for the slight underestimation of the uncertainties is due to the simplified model for calculating the distance between the photocell triggering points which do not take into account the real

[4] This correlation does not affect the individual RMSE because the 6 values used to calculate each of them originate from different runs and are uncorrelated.

shape of the car's bumper and the fact that the car has a certain slackness on the track. Slightly increasing the assumed 2 cm standard deviation of the distance along track would already be sufficient to bring the experimental values in sound agreement with the predicted ones.

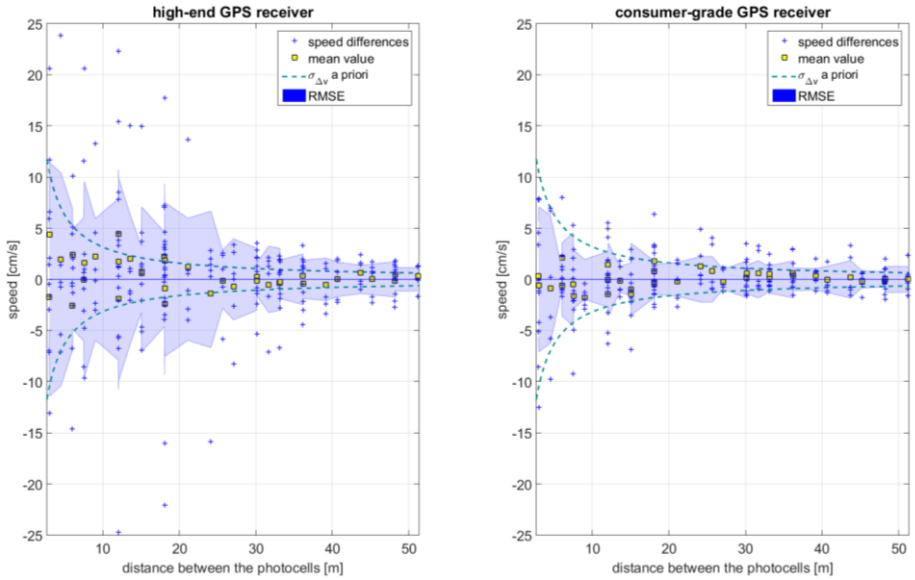

Figure 6: Differences between the velocities estimated using GNSS systems and a time cell system over different distances and the correspondent RMSE. The figure also shows the mean values of the differences as well as the a priori estimated standard deviation, calculated using (9) and assuming a mean velocity of 15 m/s. The differences and the correspondent statistics are calculated for a high-end GNSS receiver (left), as well as a consumer-grade GNSS receiver (right).

4. CONCLUSION

We have investigated the possibility of estimating the velocity using accurate GNSS Doppler observables for highly dynamic outdoor applications. We have developed a model to predict the standard deviation of speed derived by (a) GNSS and (b) photocells. Then we have carried out test measurements on a coaster track with two GNSS (in our case actually GPS) receivers/antennas mounted rigidly on the car and with track geometry and photocell positions accurately determined beforehand using a total station. Since the expected standard deviation of the photocell-based speed values exceeds that of the GNSS-based ones, it was necessary to figure the uncertainties of both in when analyzing the results.

These results indicate that indeed a precision of better than 10 mm/s is achievable for the instantaneous speed estimates of the consumer-grade GPS receiver, here taken at 5 Hz, and that these instantaneous estimates are sufficiently uncorrelated such that the precision of average speed over a certain time interval is inversely proportional to the square root of this interval. Thus accuracies on the order of a few mm/s are indeed attainable. On the other hand, the results obtained using a high-end geodetic receiver were clearly worse in the kinematic test although the receiver performs better in terms of noise by a factor of 2 during static tests.

While we used a coaster car for repeatability and control of the experiment in this study, the results are also indicative of applications where the GNSS antenna and receiver are mounted on an athlete if the body of the athlete does not obstruct the signal significantly. The impact and mitigation of such obstructions is content of future work.

REFERENCES

Boffi, G., 2013, Measurement of the center of mass kinematics in alpine skiing combining GNSS and inertial sensors, Master Thesis, EPF Lausanne.

Federolf, P. A., 2012, Quantifying instantaneous performance in alpine ski racing, Journal of Sports Sciences, 30, pp. 1063-1068.

Fontana, R., 2002, Experimental Results from an Ultra Wideband Precision Geolocation System, Proceedings of the 5th Conference on Ultra-Wideband Short-Pulse Electromagnetics, pp. 215-224.

Ford, T., Hamilton, J., 2003, A New Positioning Filter: Phase Smoothing in the Position Domain, Journal of the institute of navigation, 44, 2, pp. 65-78.

Gilgien, M.; Spörri, J.; Chardonnens, J.; Kröll, J.; Müller, E., 2013, Determination of External Forces in Alpine Skiing Using a Differential Global Navigation Satellite System, Sensors, 13, pp. 9821-9835.

Gilgien M, Spörri J, Kröll J, Crivelli P, Müller E., 2014, Mechanics of turning and jumping and skier speed are associated with injury risk in men's World Cup alpine skiing: a comparison between the competition disciplines, British Journal of Sports Medicine, 48, 9, pp. 742-747.

Gilgien, M., Spörri, J., Chardonnens, J., Kröll, J., Limpach, P., Müller, E., 2015, Determination of the Centre of Mass Kinematics in Alpine Skiing using Differential Global Navigation Satellite Systems, Journal of Sport Sciences, 33, pp. 960-969.

Gilgien M, Spörri J, Kröll J, Müller E., 2016, Effect of ski geometry and standing height on kinetic energy: equipment designed to reduce risk of severe traumatic injuries in alpine downhill ski racing, British Journal of Sports Medicine, 50, 1, pp. 8-13.

Kaplan, E.D., Leva, J.L., Milbert, D., Pavloff, M.S., 2006, Fundamentals of Satellite Navigation. In: Kaplan E.D., Hegarty, C.J. (eds), Understanding GPS: Principle and Applications, 2nd ed., pp. 21-65, Artech House Boston-London.

Klous, M., Müller, E., Schwameder, H., 2010, Collecting kinematic data on a ski/snowboard track with panning, tilting, and zooming cameras: Is there sufficient accuracy for a biomechanical analysis? Journal of Sports Sciences, 28, pp. 1345-1353.

Lachapelle, G. 2009, Ultra-precise positioning for sport applications. 13th IAIN World Congress Stockholm, pp. 1-11.

Leser, R., Baca, A., Ogris, G., 2011, Local Positioning Systems in (Game) Sports, Sensors, 11; pp. 9778-9797.

Lindinger, S., 2007, Methodological aspects in cross country skiing research. Science and Nordic Skiing, pp. 27-38, Meyer & Meyer Sport Aachen.

Nedergaard, N. J., Heinen, F., Sloth, S., Hebert-Losier, K., Holmberg, H. C., & Kersting, U., 2013, The effect of light reflections from the snow on kinematic data collected using stereo-photogrammetry with passive markers, Sports Engineering, 17, pp. 97-102.

Reid, R., 2010, A kinematic and kinetic study of alpine skiing technique in slalom, PhD Thesis, Norwegian School of Sport Sciences Oslo.

Skaloud, J, Limpach, P., 2003, Synergy of CP-DGPS , Accelerometry and Magnetic Sensors for Precise Trajectography in Ski Racing, Proceedings of the 16th International Technical Meeting of the Satellite Division of The Institute of Navigation (ION GPS/GNSS 2003), pp. 2173-2181.

Spörri, J., Kröll, J., Schwameder, H., & Müller, E., 2012, Turn Characteristics of a Top World Class Athlete in Giant Slalom: A Case Study Assessing Current Performance Prediction Concepts, International Journal of Sports Science and Coaching, 7, pp. 647-660.

Supej, M., 2010, 3D measurements of alpine skiing with an inertial sensor motion capture suit and GNSS RTK system, Journal of Sports Sciences 28, 7, pp. 759-769.

Supej, M. & Holmberg, H. C., 2011, A new time measurement method using a high-end global navigation satellite system to analyze alpine skiing, Research Quarterly for Exercise and Sport, 82, pp. 400-411.

Supej, M., Cuk, I., 2014, Comparison of Global Navigation Satellite System Devices on Speed Tracking in Road (Tran)SPORT Applications, Sensors, 14, 12, pp. 23490-23508.

Ward, P.W., Betz, J.W., Hegarty, C.J., 2006. Satellite signal acquisition, tracking, and data demodulation. In: Kaplan E.D. Hegarty, C.J., (eds) Understanding GPS: Principles and Applications, 2nd ed, pp. 153-241, Artech House Boston-London.

Wieser, A., Gaggl, M., Hartinger, H., 2005, Improved Positioning Accuracy with High-Sensitivity GNSS Receivers and SNR Aided Integrity Monitoring of Pseudo-Range Observations, Proceedings of the 18th International Technical Meeting of the Satellite Division of The Institute of Navigation (ION GPS/GNSS 2005), pp. 1545-1554.

Wieser, A., 2007, GPS based velocity estimation and its application to an odometer, Shaker Verlag Aachen.

Yeadon, M. R., Kato, T., Kerwin, D. G., 1999, Measuring running speed using photocells, Journal of Sports Sciences, 17, pp. 249-257.

Zhang, J., Zhang, K., Grenfell, R., Deakin, R., 2006, On the relativistic Doppler effect for precise velocity determination using GPS, Journal of Geodesy, 80, pp. 104-110.

BIOGRAPHICAL NOTES

Geo Boffi graduated in Geomatics and Planning at the ETH Zurich. He is research assistant and doctoral student at the Institute of Geodesy and Photogrammetry at the ETH Zurich.

Dr. Matthias Gilgien is educated in land surveying, biomechanics and sport science. His research focusses on performance enhancement and injury prevention in snow sports using navigation technology and computer simulation. He conducted research mainly for the Swiss, the Norwegian and the International Ski Federation and is Associate Professor at the Norwegian School of Sport Sciences.

Dr. Andreas Wieser is a full professor of Geosensors and Engineering Geodesy at the ETH Zürich. He has over 15 years of experience in academic research and teaching from various positions held at the Vienna University of Technology, the Graz University of Technology and the University of Calgary. His research interests are geodetic monitoring, high precision positioning, kinematic surveying, parameter estimation and quality control.

ACKNOWLEDGMENTS

The authors thank Pascal Inauen for his contributions to the field work and some of the data processing underling the study.

CONTACTS

Geo Boffi
Institute of Geodesy and Photogrammetry, ETH Zurich
Stefano-Franscini-Platz 5
8093 Zurich / Switzerland
Phone +41 44 633 32 56
Fax +41 44 633 11 01
geo.boffi@geod.baug.ethz.ch
http://www.gseg.igp.ethz.ch/

Matthias Gilgien
Department of Physical Performance, Norwegian School of Sport Sciences

P.o. box 4014 Ullevål Stadion
0806 Oslo / Norway
Phone: +4745676656 / +41795330191
matthias.gilgien@nih.no
http://www.nih.no/om-nih/organisasjon/ansatte/gilgien-matthias/

Andreas Wieser
Institute of Geodesy and Photogrammetry, ETH Zurich
Stefano-Franscini-Platz 5
8093 Zurich / Switzerland
Phone +41 44 633 0555
Fax +41 44 633 11 01
andreas.wieser@geod.baug.ethz.ch
http://www.gseg.igp.ethz.ch/